New Innovations in Chemistry and Biochemistry

Vol. 6

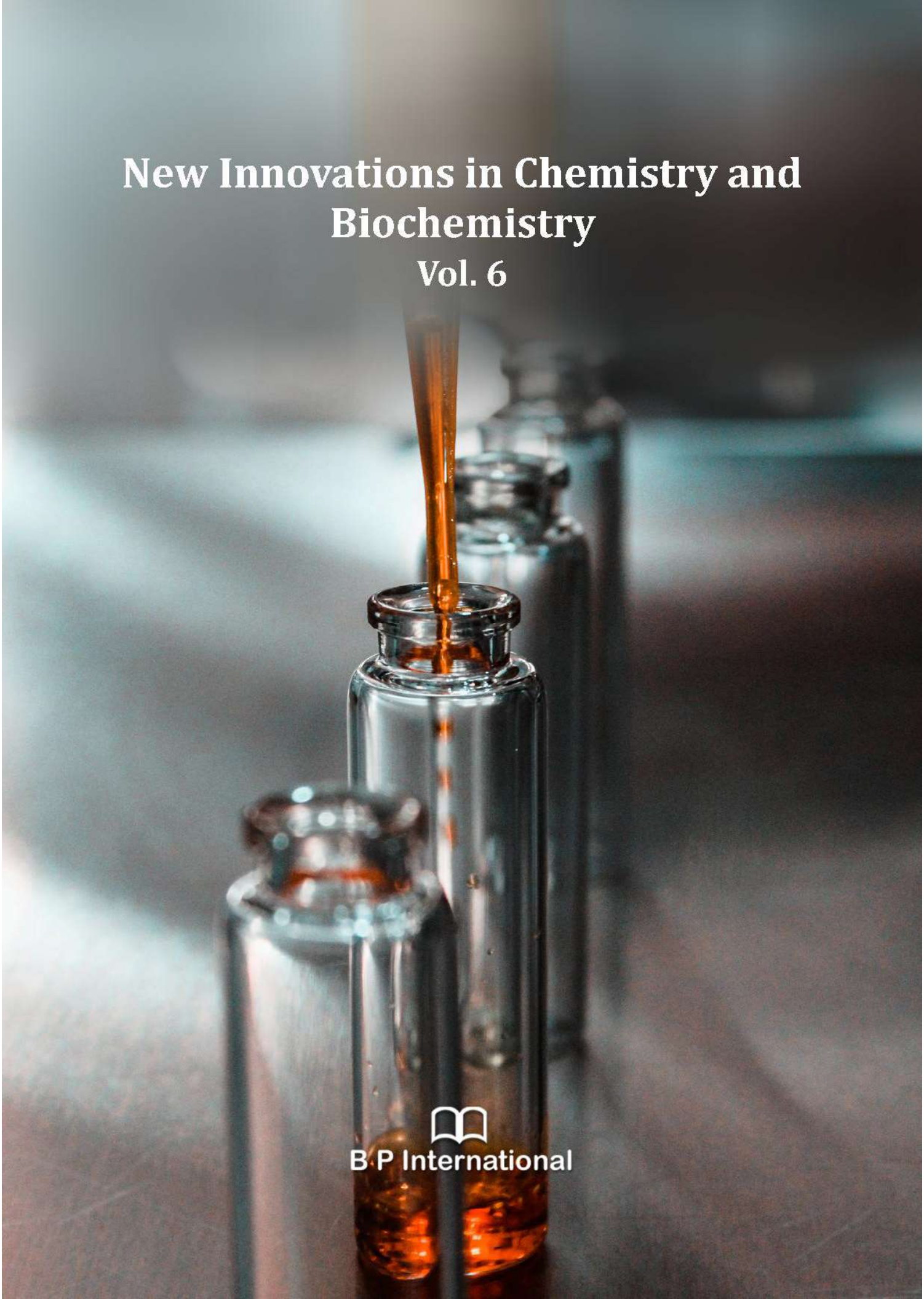

B P International

New Innovations in Chemistry and Biochemistry

Vol. 6

New Innovations in Chemistry and Biochemistry

Vol. 6

India ▪ United Kingdom

B P International

Editor(s)

Dr. Pradip K. Bhowmik

Professor,
Department of Chemistry and Biochemistry, University of Nevada Las Vegas, Nevada, USA.
Email: pradip.bhowmik@unlv.edu;

FIRST EDITION 2021

ISBN 978-93-5547-091-1 (Print)
ISBN 978-93-5547-143-7 (eBook)
DOI: 10.9734/bpi/nicb/v6

Contents

Chapter 2
Print ISBN: 978-93-5547-091-1, eBook ISBN: 978-93-5547-143-7

Transition Metal Doped Nanocrystalline MgO Catalyzed Green Chemical Synthesis of E-Ethyl Cinnamate Using One Pot Wittig Reaction

Mansur Moulavi [a*] and Kaluram Kanade [b]

DOI: 10.9734/bpi/nicb/v6/1673A

ABSTRACT

Ethyl cinnamate is important chemical produced by industries on commercial scale. Although this is available naturally in number of plants, the cost of extraction and purification is non-affordable on commercial scale. Existing method for syntheses of this chemicals are acid and enzymatic esterification as well as condensation using Na metal and strong bases under homogeneous condition. These methods are limited by low yield, long reaction time and pollution on commercial scale. To circumvent these limitations, it is very important to develop the method for synthesis of ethyl cinnamate under heterogeneous condition using reactive catalytic systems. For this purpose, Cu, Fe, and Mn doped nanocrystalline MgO was synthesized using an alkali leached hydrothermal technique and used as heterogeneous basic catalysts in a one-pot Wittig reaction to produce ethyl cinnamate. XRD, UV-DRS, FT-IR, FESEM, EDS, and XPS techniques are used to characterize the basic catalysts. The catalytic activity of synthesised catalysts was investigated in a one-pot Wittig reaction at room temperature in DMF solvent of benzaldehyde, triphenylphosphine, and ethyl bromoacetate. Under optimised reaction conditions, the Mn doped nanocrystalline MgO catalyst yields 98 percent. Enhancement of surface basicity due to doping of Mn in MgO was ascertained by UV-DRS and XPS study. In this study we observed the synergistic effect of transition metal doping, particle size and morphology on surface basicity enhancement of nanocrystalline MgO in one pot Wittig reaction for green chemical synthesis of ethyl cinnamate.

Keywords: Nanocrystalline MgO; green chemical synthesis; ethyl cinnamate.

1. INTRODUCTION

Naturally occurring ethyl cinnamate ester is well known flavoring agents mixed in large number of food stuff having cinnamon, strawberry, raspberry, plum, cherry and other types of flavors. High thermal stability allows its use in baked goods. In addition to this, it is used in many commercial products including soap, medicines and ointments [1]. The low concentration of these esters in plants like *Kaempferia galangal* etc. and cost of extraction, separation and purification restricts the production and utilization on commercial scale [2]. Chemical synthesis finds the suitable way for synthesis of cinnamate ester flavoring agent. The earlier synthetic methods including acid and enzyme catalyzed esterification of ethyl alcohol with cinnamic acid, Claisen ester condensation, $POCl_3$ and enzymatic method under homogeneous environment results for extreme acidic condition, use of hazardous chemicals, high temperature and very longer reaction time with poor yield so environmentally and economically not viable [3]. Heterogeneous reactions using oxide based solid basic systems find the easier ways for this purpose [4].

Among the heterogeneous catalysis, several base catalyzed C-C bond forming organic reactions such as Aldol condensation [5] Knoenvengal condensation [6] Claisen Schmidt condensation [7] Biginilli

[a] *Department of Chemistry, PDEA's Annasaheb Waghire College, Otur, Pune -412409, India.*
[b] *Annasaheb Awate Arts, Commerce, Hutatma Babu Genu Science College, Manchar Pune-410503, India.*
**Corresponding author: E-mail: mhmoulavi251985@gmail.com;*

reaction [8] and coupling reactions [9] are well known. These heterogeneous organic reactions are catalyzed by MgO, ZnO, CaO, SrO, and TiO_2 catalysts via a green chemical approach [10]. Among these solids, MgO is used as a base catalyst. It is very cheap, easily available and recyclable catalyst [11]. Wittig reaction is one of the stereo-selective methods for preparation of olefin from aldehydes or ketones [12]. This important C-C bond forming reaction generally comprises two steps under homogenous basic conditions using NaOH, KOH, $Ba(OH)_2$, alkoxides, hydrides [13] It suffers from many drawbacks such as drastic reaction conditions, contamination of products and excessively strong basic conditions. Thus, it requires huge amount of solvent for purification and vice versa unwanted separation. To overcome this, Wittig reaction can be made to operate in one pot without isolation of intermediate phosphonium salt and phosphorus ylide under heterogeneous mild reaction condition using nanocrystalline MgO. However, this heterogeneous basic condition requires longer reaction time [14,15]. Hence many researchers are ensuing efforts in order to develop and modify the basicity of MgO for such organic reactions [16-21]. The existence of low coordinated acidic and basic sites on surface and corners of MgO have been reported towards active interactions of catalysts with acidic and basic parts of organic molecules [22]. It has been successfully demonstrated that low coordinated Mg^{2+} ions at surface and corners act as acidic sites, while low coordinated oxygen anions act as basic site. The 3 coordinated oxygen anions on surface are found to be most reactive [23]. Generally basic strength of basic sites varies in order $O^{2-}_{3C} > O^{-2}_{4C} > O^{-2}_{5C} > O^{-2}_{6C.}$ [24]. Thus basic site on the surface of MgO was found responsible for heterolytic cleavage of organic molecules. In this way, surface basicity of MgO plays a key role in proceeding organic reactions. It is also noticed that surface basicity of MgO can be changed by doping other ions in crystal structure of MgO [25]. Doping of MgO with metal ions not only changes its electronic properties [26] but also increases number of active basic sites on surface [27].

In the present communication, we report the synthesis of pure undoped nanocrystalline and Cu/Fe/Mn doped MgO catalysts. In particular, the effect of particle size, morphology and doping of metal ions on basicity has been investigated in the context of the reported one pot Wittig reaction. The combined effect of doping transition metal in MgO and nano-particulate nature and morphology exerts the synergistic effect on surface basicity enhancement which is evidently beneficial for catalytic application in synthesis of E-ethyl cinnamate using one pot Wittig reaction.

1.1 Objectives of Study

Replacement of existing reactive, corrosive reaction conditions for synthesis of E-ethyl cinnamate

1) Syntheses and characterization of Cu, Fe and Mn ions doped nanocrystalline MgO catalysts.

2) Evaluating and comparing the catalytic activity of Cu, Fe and Mn ions doped nanocrystalline MgO in one pot Wittig reaction.

3) Optimization of reaction parameters of one pot Wittig reaction for green chemical syntheses of E-ethyl cinnamate using Transition Metal Doped Nanocrystalline MgO Catalysts.

2. EXPERIMENTAL

2.1 Methods

2.2.1 Preparation of nanocrystalline MgO Catalyst

5 g commercial MgO powder was added with stirring to 100 mL 10 M NaOH in 200 mL capacity teflon reactor with stainless still outer jacket. It was then subjected to alkali leached hydrothermal reaction at 180 °C for 24 h. After cooling, the resulting $Mg(OH)_2$ was transferred to 500 mL water in a beaker. It was further diluted and washed with 20 liter deionised water and excess alkali was neutralized with very dilute HCl. This content is filtered with suction pump using whatmann filter paper no 41 and dried at 60 °C for 6 h. The magnesium hydroxide obtained by this treatment, was calcined at 450 °C to obtain the nanocrystalline MgO catalyst [28].

2.2.2 Preparation of nanocrystalline 1 wt % Cu, Fe, Mn doped MgO catalysts

For the preparation of 1 wt % Cu, Mn and Fe doped nanocrystalline MgO, the desired stoichiometric quantity of each copper chloride dihydrate, manganese chloride tetra hydrate and ferrous sulphate heptahydrate was taken respectively and ground with 5 g commercial MgO for 1 h in a mortar with pestle and each Cu, and Fe and Mn doped crushed MgO samples were subjected to alkali leached hydrothermal method at 180°C for 24 h. After alkali treatment, the resulting Cu, Fe and Mn doped $Mg(OH)_2$ was transferred to 500 mL water in a beaker. It was further diluted and washed with 20 liter deionised water and excess alkali was neutralized with very dilute HCl. This content is filtered with suction pump using whatmann filter paper no 41 and dried at 60°C for 6 h. The Cu, Fe and Mn doped magnesium hydroxide obtained by this treatment, was calcined at 450°C to obtain 1 wt% Cu, Fe and Mn doped nanocrystalline MgO.

2.2.3 Synthesis of E-ethyl cinnamate using transition metal doped MgO catalysts in one pot Wittig reaction

(4.7 mmol) benzaldehyde, (4.7 mmol) triphenylphosphine and (4.7 mmol) ethyl bromoacetate were stirred in 5 mL DMF with each catalyst in 25 mL small round bottom flask under ambient conditions. The completions of reactions were monitored by TLC technique using 80% hexane: ethyl acetate mobile phase. After completion of reaction, DMF solvent was added in the reaction mixture and the catalyst was separated by centrifugal separation at 5000 rpm. The separated catalysts were washed with DMF and ethyl acetate and again heated for the next cycle. Reaction mixture was subjected to work up with water and ethyl acetate to remove excess of DMF. The products olefin and triphenylphosphine oxide were purified and separated on silica loaded column using pure hexane as eluent.

The product of Wittig reaction was characterized by High Resolution-Mass Spectra (HR-MS), ^{1}H-NMR and ^{13}C-NMR technique. For characterization of Wittig reaction product ethyl cinnamate, HR-MS was taken on Bruker Compass Data Analysis 4.2. ^{1}H-NMR analysis of products was carried out using Bruker model.

3. RESULTS AND DISCUSSION

Synthesis of undoped nanocrystalline MgO and Cu/Fe/Mn doped has been carried out using alkali leached hydrothermal method as stated in experimental section. As-synthesized product materials were characterized by using XRD, UV-DRS, FT-IR, FESEM, EDS and XPS analysis.

3.1 X-Ray Diffraction Analysis

3.1.1 XRD analysis of commercial MgO, $Mg(OH)_2$ and nanocrystalline MgO

Fig. 1 shows the XRD patterns of commercial MgO, magnesium hydroxide and nanocrystalline MgO. The XRD pattern of commercial MgO (Fig. 1a) shows impurity peaks of $Mg(OH)_2$ at 2θ values 18.50, 37.94, 58.55, while remaining peaks reveal the cubic phase of MgO (JCPDS file no 44-1482). XRD pattern in **(1b)** demonstrates that XRD peaks mostly match with $Mg(OH)_2$ as evidenced by 2θ values at 18.52, 32.89, 37.99, 50.86, 58.63, 62.05, 68.32 and 72.04 degrees which respectively correspond to 001, 100, 101, 102, 110, 111, 103, 201 planes of hexagonal crystal system of $Mg(OH)_2$ brucite phase (JCPDS file no 44-1482). The conversion of cubic MgO to hexagonal nanocrystalline $Mg(OH)_2$ can occur due to the leaching effect of highly concentrated alkali in hydrothermal synthesis. However, we intended to synthesize pure nanocrystalline MgO and hence, the as-synthesized $Mg(OH)_2$ was further calcined at 450°C. At 450°C, the hexagonal $Mg(OH)_2$ gets completely converted to cubic MgO (Fig. 1c). The observed 2θ values of XRD pattern (Fig. 1c) at 36.91, 42.88, 62.29, 74.68, and 78.61 degrees corresponding to planes 111, 200, 220, 311, 222 matched well with cubic phase of MgO (JCPDS file no 45-0946). Highly pure nanocrystalline cubic phase of MgO synthesized in this way has been subsequently used for transition metal doping and catalytic study.

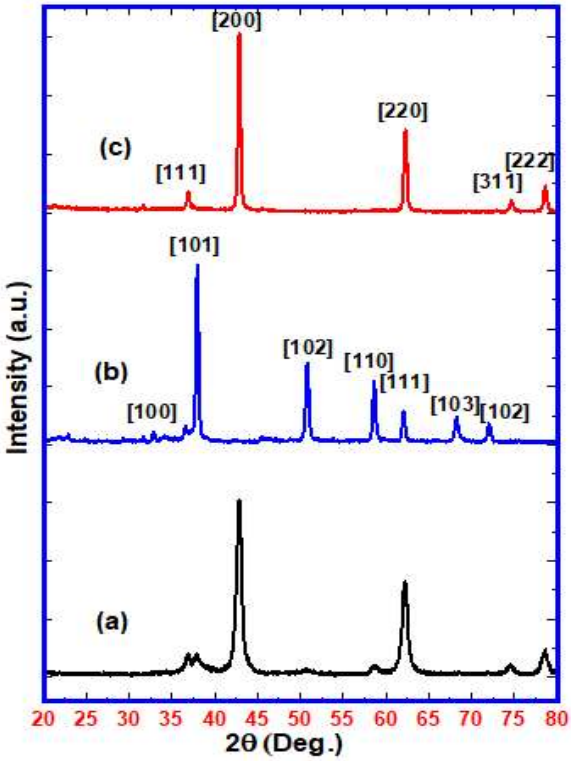

Fig. 1. XRD patterns of (a) Commercial MgO (b) $Mg(OH)_2$ (c)Synthesized nanocrystalline MgO

3.1.2 Effect of calcination temperature on crystallite size of nanocrystalline MgO

Fig. 2 displays the X-ray diffraction patterns of nanocrystalline MgO calcined under different temperatures viz. 450°C, 700°C and 900°C. For surface activation of MgO and for tuning of crystallite size, calcination at suitable temperature is recommended [29,30]. The average crystallite sizes for nanocrystalline MgO particles were calculated for different calcination temperatures by using Scherer's equation at [200] plane. Under no activation (i.e no heating) condition, although the commercial MgO disclosed smallest crystallite size, it indicated presence of surface hydroxide impurity. On raising the calcination temperature from 450 °C to 700 °C, the crystallite size appears to be reduced from 26 nm to 17 nm. Apparently, we observed the smallest crystallite size for the sample calcined at 700°C for 4 h calcination time. On increasing the calcination temperature up to 900°C, crystallite size appears to increase again. The observed irregularity in crystallite size variation as a function of calcination temperature may be attributed to changing crystallinity pattern and intrinsic defects [31]. Thus, the calcination temperature 700 °C was found to be optimum for surface activation as it yields smallest crystallite size.

3.1.3 XRD Analysis of 1 wt% Cu/Fe/Mn doped MgO

Fig. 3 shows the XRD patterns corresponding to pure (undoped) nanocrystalline MgO, 1 wt% Cu doped MgO, 1 wt% Fe doped MgO and 1 wt% Mn doped MgO. All XRD peaks are in agreement with JCPDS values for cubic phase of MgO (JCPDS file no 45-0946). The effect of doping by Cu, Fe and Mn in nanocrystalline MgO has not been predominantly observed as expected in terms of shifting of the peaks. The average crystallite size calculated by using Scherer's equation at [200] plane is observed in the range of 16 to 19 nm. The undoped nanocrystalline MgO and 1 wt% Fe doped nanocrystalline MgO catalysts show the crystallite size of 17 nm. 1 wt% Cu doping in nanocrystalline MgO leads to crystallite size of 19 nm for the resultant catalyst sample while 1 wt% Mn doping in nanocrystalline MgO leads to smallest crystallite size of 16 nm for the resultant catalyst sample. For the measurement of the catalytic efficiency, 1 wt% Cu, Fe and Mn doped nanocrystalline MgO samples were used.

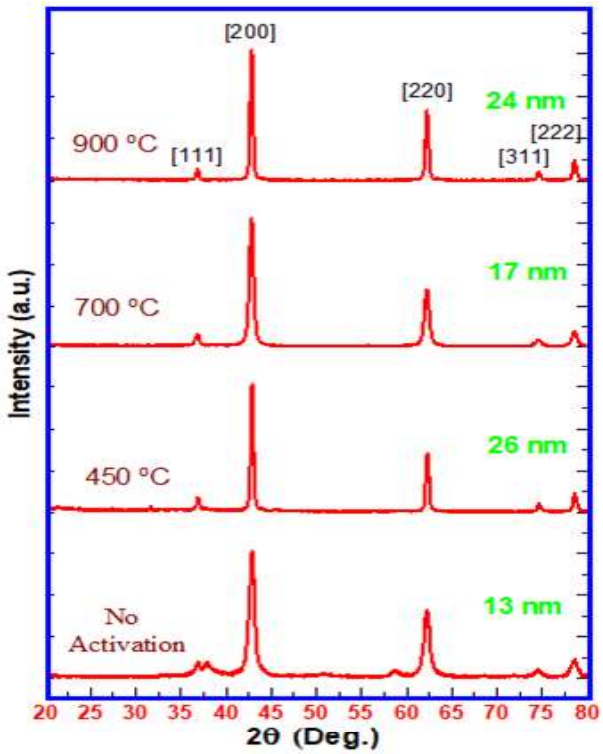

Fig. 2. Effect of calcination temperature on crystallite size of nanocrystalline MgO

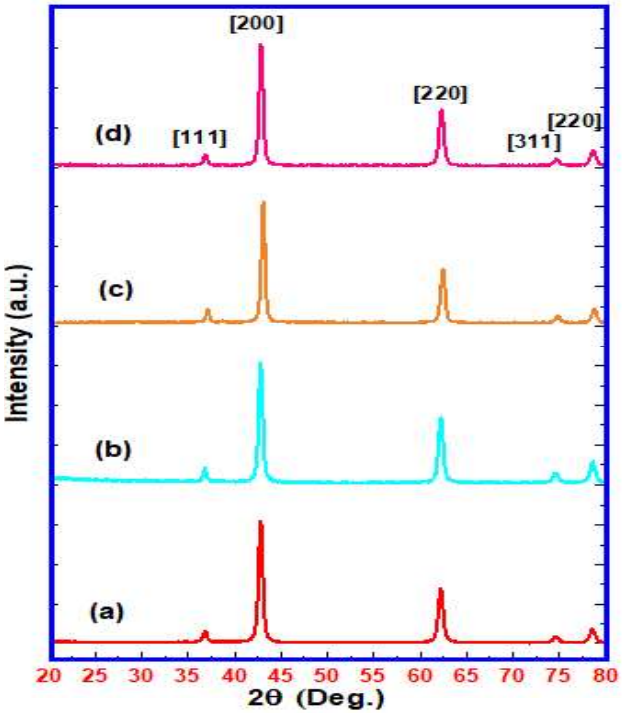

Fig. 3. XRD patterns of (a) Nanocrystalline MgO, (b) 1 wt% Cu doped MgO (c) 1 wt% Fe doped MgO and (d) 1 wt % Mn doped MgO catalysts calcined at 700°C

3.2 UV-Diffused Reflectance Analysis

Fig. 4 displays the UV diffused reflectance spectra of undoped and 1 wt% Cu/ Fe/Mn doped MgO nanomaterials. Undoped nanocrystalline MgO reveals formation of pure phase (Fig. 4a) with absorption band around 274 nm. In case of 1 wt% Fe doped MgO sample, absorption band exhibits red shift at 347nm (Fig. 4b). In case of 1 wt% Cu doped MgO sample, two sharp absorption bands at 230 nm and 274 nm are observed along with red-shifted band at 552 nm (Fig. 4c). Similarly, for 1 wt % Mn doped MgO sample, two absorption bands (located at 228 nm and 281 nm) as well as one red-shifted band (located at 482 nm) have been noticed(Fig. 4d). These multiple sharp absorption bands in UV-DRS spectra form an important tool for gaining an insight into distribution of surface basicity of MgO [30] Fig. 4c and 4d illustrate multiple absorption bands in UV-DRS of 1 wt% Cu and Mn doped MgO nanocrystalline materials. The absorption bands mainly at 228 and 281 nm may be related to low coordinated oxygen at surface, corners and kinks of MgO system as reported by Zhang et al. [31].

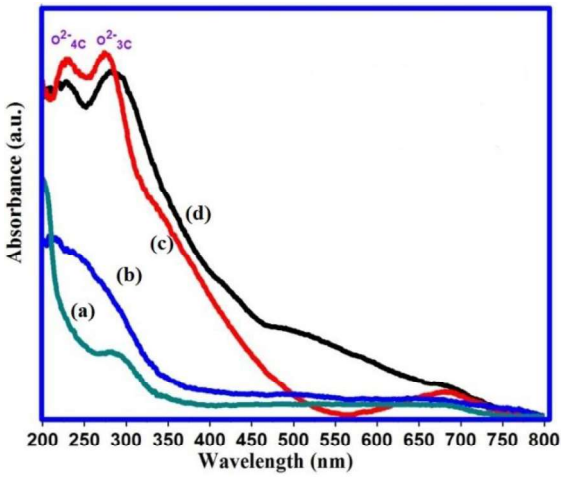

Fig. 4. UV-DRS spectra of (a)undoped nanocrystalline MgO (b)1 wt% Fe doped MgO (c)1 %wt Cu doped MgO and (d)1 %wt Mn doped MgO

The strength and number of this low coordinated oxygen is responsible for the enhancement of surface basicity. It is also reported that UV absorption at 280 nm corresponds to excitation of 3 coordinated oxygen atom at surface and UV absorption at 230 nm is associated with excitation of 4 coordinated oxygen [32].

In our case, similar absorption bands for undoped, Cu doped and Mn doped MgO materials are observed implying presence of low coordinated oxygen yielded in Cu and Mn doped nanomaterials which, in turn, can effectively enhance the catalytic efficiency for the proposed reaction. The Fe doped MgO nanomaterial does not show any absorption band. It indicates the absence of low coordinated oxygen at surface probably due to preferential formation of Fe-O interface bias layer on the surface of FeO as reported earlier [33]. Overall UV-DRS study shows that the proposed methodology for synthesis of transition metal doped MgO has certain intrinsic advantages, which might be beneficial to increase number of low coordinated oxygen in Cu and Mn doped MgO nanomaterial. Hence, as-synthesized doped MgO nanomaterials were further used as heterogeneous basic catalysts in reported one pot Wittig reaction.

3.3 Fourier Transform Infra-Red Analysis

Fig. 5 shows the FT-IR spectra of nanosized undoped and 1 wt% Cu/Fe/Mn doped MgO catalysts. It is fairly established that FT-IR analysis is an important tool to obtain information about nature of surface oxygen in MgO [34]. The similar absorption regions for Mg-O stretching frequencies are observed in the range of 400-850 cm^{-1} (Fig. 5). In the first region, the bands due to different

fundamental Mg-O vibrations are observed between 400-500 cm^{-1} [35]. In the second region, combination bands of fundamental vibrations appeared between 550-850 cm^{-1} [36]. Two bands appeared between 1400-1500 cm^{-1} in all undoped and Cu/Fe/Mn doped nanosized catalysts indicating the adsorption of CO_2 on MgO surface as reported previously [37]. In case of Fe doped MgO catalyst, these absorption bands are significant which might be due to adsorption of CO_2 and its spongy nature as observed in FESEM photographs. Absence of bands in the region 3400-3600 cm^{-1} specifies the purity of material.

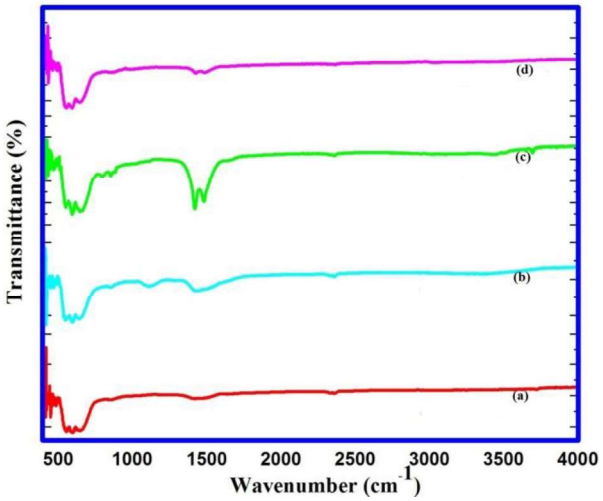

Fig. 5. FT-IR spectra of (a) nanocrystalline MgO(b)1 wt% Cu doped MgO (c)1 wt% Fe doped MgO and (d)1 wt% Mn doped MgO

3.4 Field Emission Scanning Electron Microscopic Analysis

Fig. 6 presents FESEM photographs of pure and doped nanocrystalline MgO catalysts which, by and large, disclose formation of hexagonal plates. The average particle size of hexagonal plates of nanocrystalline MgO is 68 nm and thickness appears to be 18 nm (Fig. 6a,6b). The 1 wt% Fe/MgO catalyst shows spongy/porous hexagonal plates with the average particle size of 240 nm, thickness of 32 nm and average pore size of 10 nm (Fig. 6c,6d). The hexagonal plates of 1 wt% Cu/MgO show average particle size of 450 nm and thickness of 70 nm (Fig. 6e,6f). The 1 wt% Mn/MgO catalyst displays formation of nanosheets and spherical particles. The thickness of nanosheet is 21 nm while the length and breadth are in the order of micron size. The spherical particles of 1 wt% Mn/MgO catalyst indicate average diameter of 180 nm (Fig. 6g,6h). All these FESEM observations confirm formation of nanomaterials with distinct morphology.

3.5 Energy Dispersive X-Ray Spectroscopy (EDS) for Elemental Analysis

Fig. 7 furnishes typical EDS elemental analysis data for 1 wt% Cu, 1 wt% Fe and 1 wt% Mn doped MgO catalysts. The recorded spectra endorse presence of Cu, Fe and Mn metal in MgO material. In case of Cu doping in MgO, the normalized weight % for Cu is found to be 1.02% (Fig. 7a) while for Fe doped MgO, the normalized weight % for Fe is found to be 0.73 % (Fig. 7b) and in case of Mn doped MgO, the normalized % weight for Mn is found to be 1.34 % (Fig.7c). The pertinent EDS data evinces that doping of transition metals in nanocrystalline MgO matrix takes place successfully.

3.6 XPS Analysis

X-ray photoelectron spectroscopic analysis was performed for identification of oxidation state of catalyst elements and to determine the strength of basic catalysts. Fig. 8 furnishes the XPS scans displaying binding energy (BE) peaks (deconvulated) for Mg 2P and O 1S energy states in pure

nanocrystalline MgO and 1 wt% Cu, Fe and Mn doped MgO. After carbon correction, binding energy values for Mg 2P energy states are observed at 49.8, 49.6, 49.4 and 48.8 eV respectively. In case of XPS peak of O1S energy state, each peak is deconvulated into three peaks. The smallest value peak represents lattice oxygen, middle value peak represents surface hydroxides and largest value peak represents the surface carbonates. Accordingly, lattice oxygen XPS peaks for pure, Cu, Fe and Mn doped MgO catalysts are observed at 529.6, 529.3, 528.92 and 529.6 eV respectively (Fig. 8a-8d). In XPS analysis, binding energy of $2P_{3/2}$ energy state is very important diagnostic peak for distinguishing different oxidation states of transition metals. Fig. 9 provides XPS scans showing BE peaks for $2P_{3/2}$ and $2P_{1/2}$ energy states of Cu, Fe and Mn elements in doped MgO catalysts (Fig. 9a-9c). It may be recalled that all pure undoped and doped nanocrystalline MgO catalysts are calcined at 700 ^{O}C. In the context of XPS analysis in Fig. 9, for Fe doped MgO catalyst, the XPS peak at 709.4 might be ascribed to presence of Fe (II) in MgO (Fig. 9a). The binding energy peaks of $2P_{3/2}$ energy states appeared at 932.7 eV might be ascribed to presence of Cu (II) which is strongly distinguished from Cu (I) and Cu(0) by presence of strong Cu (II) satellite peak at 940.4 eV (Fig. 9b). The presence of XPS peak at 641.8 eV is ascribed for Mn (IV) in MgO catalyst (Fig. 9c). Doublet at this position confirms the absence of other oxidation state of Mn in MgO [Vasquez [38], Mansour and Brizzolara [39], Nesbitt and Banergee[40] and Stranick [41]. It is worthwhile to note that at higher calcination temperature under oxidising condition, Mn exists in higher oxidation state in MgO.

High resolution XPS scans corresponding to Mg 2p and O 1s energy states of pure and doped MgO catalysts elucidate that doping of Cu, Fe and Mn elements in MgO can cause shifts in pertinent binding energy values presumably due to change in surface basicity. On the contrary, surface basicity of MgO like solid bases can be correlated with binding energy of O 1S energy states [42].

As a general rule, low binding energy values of O 1S energy state increases the surface basicity and vice versa [43]. Qualitatively, it is very difficult to predict the surface basicity of surface oxygen just by looking at increase or decrease of binding energy values of O 1S energy states, rather relative binding energy difference (**ΔB.E)** between O 1S and Mg 2P energy states and binding energy shifts [2] are useful for comparative evaluation of surface basicity values of the same basic catalysts. Table 1 illustrates the relative binding energy difference between O 1S and Mg 2P energy states and binding energy shift for pure and Cu, Fe and Mn doped MgO basic catalysts calcined at 700 $^{\circ}$C.

Table 1. Relative binding energy difference and binding energy shift between O 1S and Mg 2P energy levels in 1 wt% Cu, Fe and Mn doped nanocrystalline MgO

No	Catalysts	Binding energy eV			Shift in B. E.
		O1S	Mg2P	ΔB.E	
1	Nanocrystalline MgO	529.6	49.8	479.8	0.0
2	1 wt% Cu/MgO	529.3	49.6	479.7	+0.1
3	1 wt% Fe/MgO	528.92	49.4	479.52	+0.28
4	1 wt% Mn/MgO	529.6	48.8	480.8	-1.0

From shifts in binding energy values as stated in Table 1, it is seen that binding energy of 1 wt% Cu doped MgO basic catalyst is increased by only 0.1 eV while for 1 wt% Fe doped MgO it is increased by 0.28 eV. Interestingly, 1 wt% Mn doping in MgO shows drastic decrease in binding energy by 1.0 eV. From such observations, it is argued that doping of 1 wt% Mn in MgO leads to enhancement of surface basicity of MgO catalyst compared to that of 1 wt% Cu and Fe doped MgO catalysts. As doping of Cu and Fe is responsible for increasing the binding energy of MgO system, this increased and decreased charge of Mg and O must be compensated by transition metal dopant in MgO crystallites. These elements after doping exist in oxide forms. Hence, this charge compensation can be calculated by considering again relative binding energy difference of transition metal ions $2P_{3/2}$ and O 1S energy states and binding energy shifts between standard CuO, FeO and MnO_2 with that of observed for the same doped elements in MgO. Table 2 shows the relative binding energy difference of $2P_{3/2}$ and O 1S energy states and binding energy shift for standard corresponding oxides with that of the observed ones.

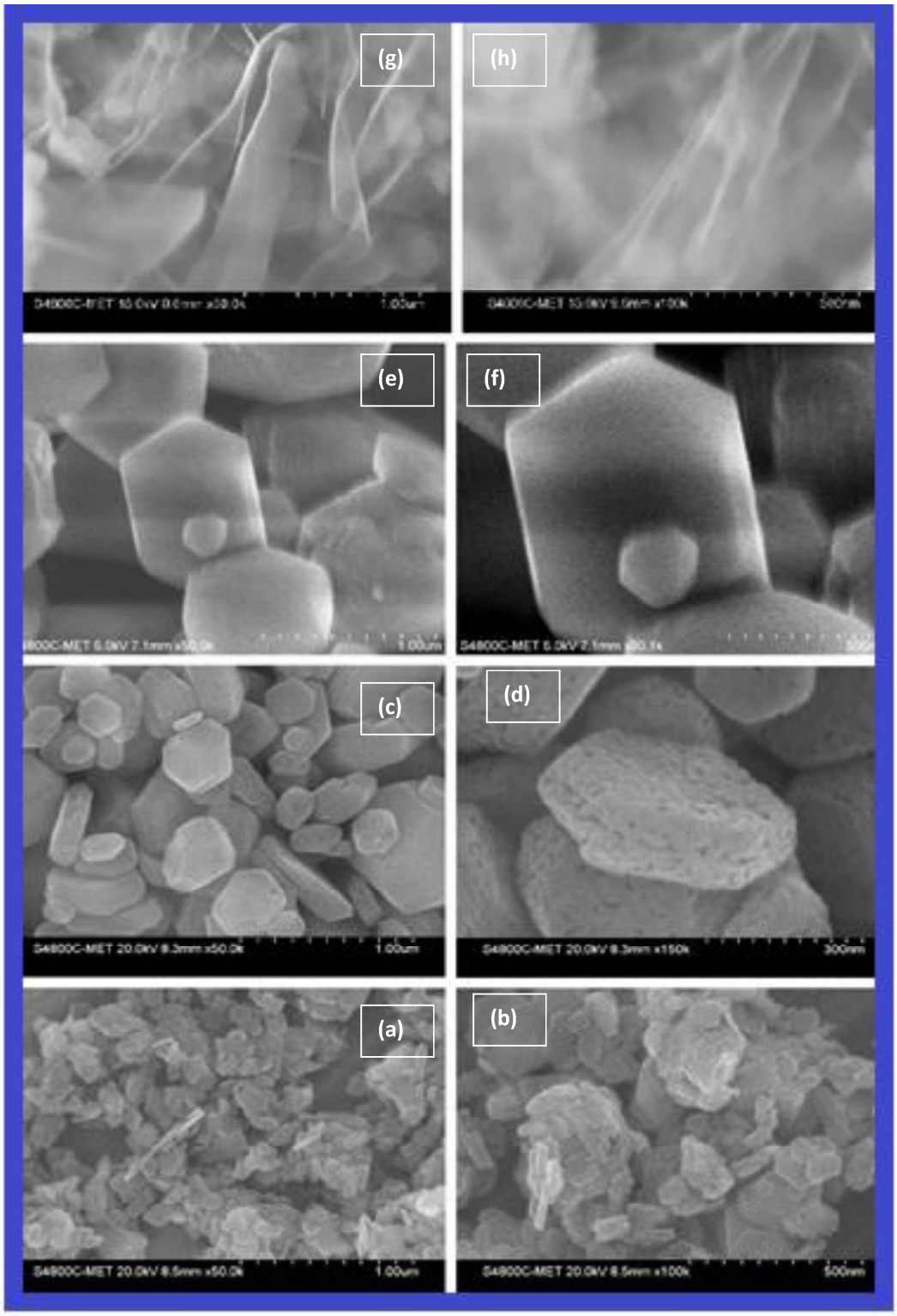

Fig. 6. FESEM images of (a-b) Nanocrystalline Pure MgO, (c-d) 1 wt % Fe doped MgO, (e-f) 1 wt% Cu doped MgO, (g-h) 1 wt% Mn doped MgO

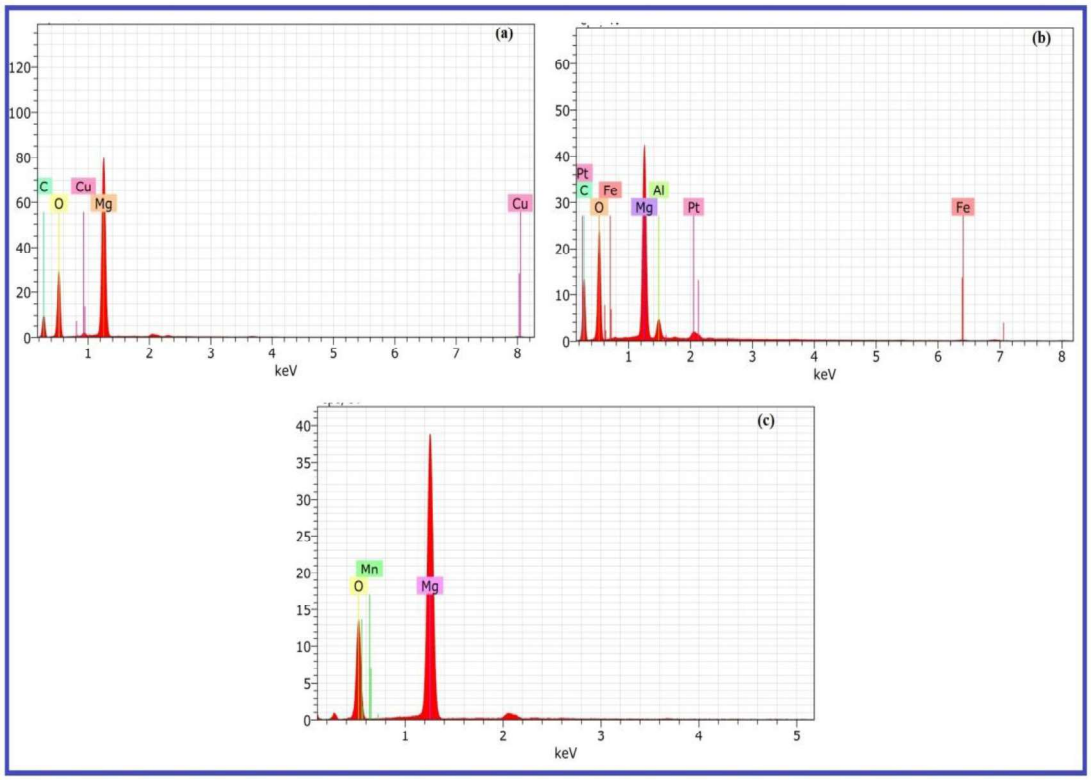

Fig. 7. EDS Elemental Analysis of (a)1 wt% Cu doped MgO, (b)1 wt% Fe doped MgO and (c)1 wt% Mn doped MgO

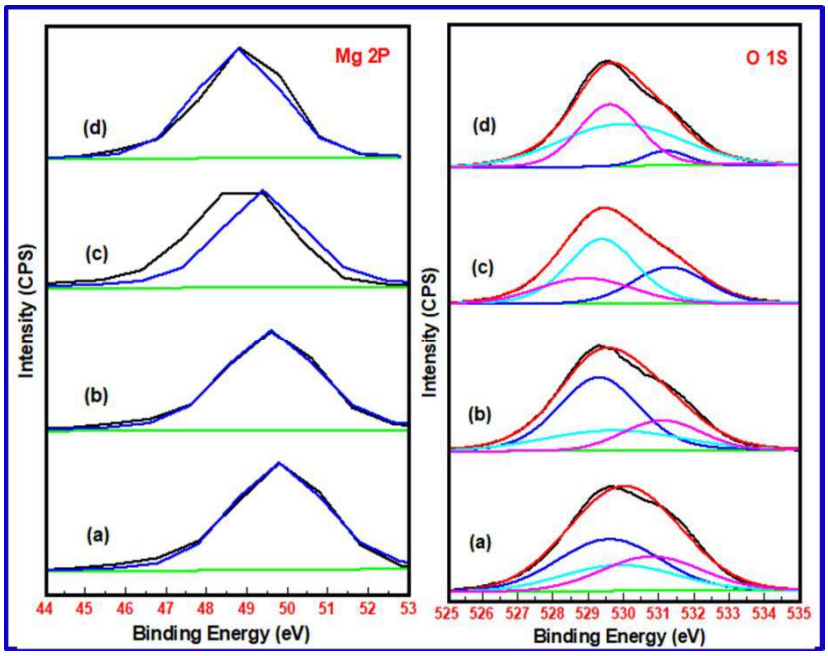

Fig. 8. XPS Scans of Mg 2P and O 1S energy states in a) pure nanocrystalline MgO b)1wt% Cu doped MgO c)1wt% Fe doped MgO d)1wt% Mn doped MgO

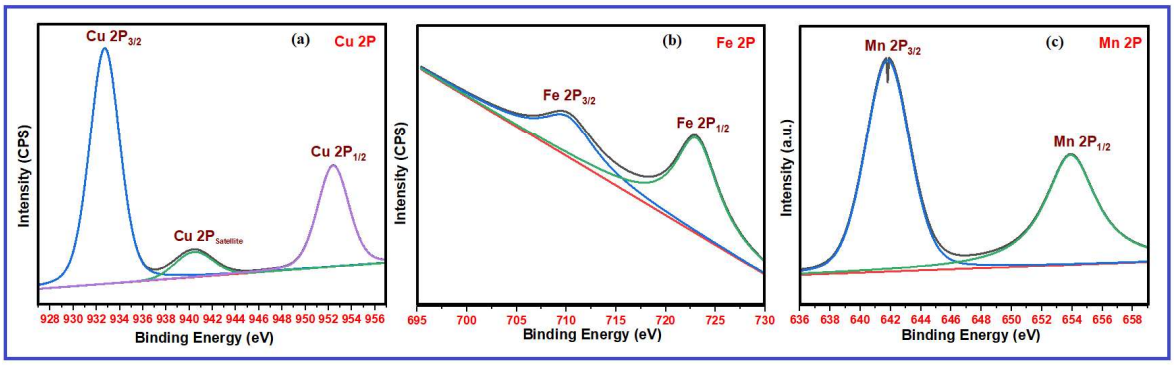

Fig. 9. XPS scans corresponding to 2P energy states in a) 1wt% Cu doped MgO b)1wt% Fe doped MgO c)1wt% Mn doped MgO

Table 2. Relative binding energy difference between $2P_{3/2}$ and O 1S energy levels and binding energy shift in standard corresponding oxides with reference to observed ones

No.	Samples	Binding energies of oxides eV				Binding energy difference eV		B. E. Shift
		Standard		Observed		Standard	Observed	
	Energy states	$2P_{3/2}$	O 1S	$2P_{3/2}$	O 1S	$2P_{3/2}$	O 1S	
1	1 wt% Cu/MgO	933.45	529.40	932.7	529.3	404.05	403.4	+0.65
2	1 wt% Fe/MgO	710.1	529.60	709.4	528.92	180.5	180.48	+0.02
3	1 wt% Mn/MgO	642.4	529.60	641.8	529.6	112.8	112.2	+0.6

From Table 2, it is reflected that although binding energy of MgO in 1 wt% Cu and Fe doped MgO increases, this charge is not compensated by dopant Cu and Fe in MgO matrix, while binding energy of MgO in 1 wt% Mn doped MgO decreases. This increased charge of Mg and decreased charge of O elements are compensated by Mn under oxidising environment. Due to higher variable oxidation state of Mn in MgO, decrease in binding energy of MgO is significant and this charge is considerably compensated. From the XPS analysis, it is confirmed that higher oxidation state Mn (IV) is responsible for enhancement of surface basicity of MgO basic catalyst by the virtue of surface electron donor characteristic attributed to variable oxidation state.

3.7 Synthesis of E-ethyl Cinnamate Using Transition Metal Doped Nanocrystalline Mgo in One Pot Wittig Reaction

In the present work, we report an efficient one-pot, three component Wittig reaction for the synthesis of ethyl cinnmate in the presence of nanocrystaline MgO (undoped and Cu, Fe, Mn doped) as highly effective heterogeneous base catalysts at room temperature **(Scheme 1).** This protocol involves synergistic effect of doping transition metals in crystal structure of MgO and nanocrystalline size in enhancing the surface basicity of MgO for one pot Wittig reaction.

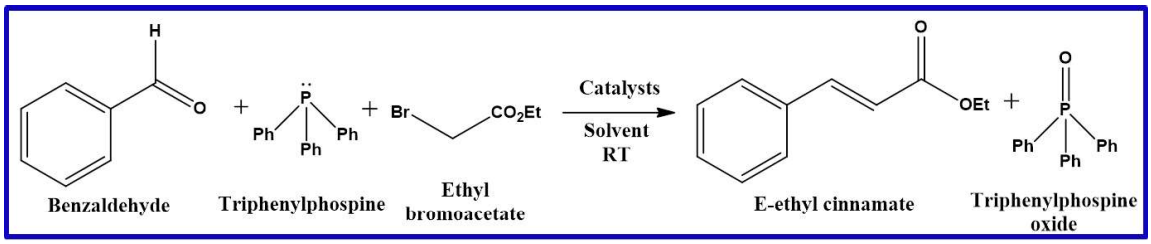

Scheme1. One pot Wittig reaction of benzaldehyde, triphenylphosphine, ethyl bromoacetate in presence of MgO catalysts

3.7.1 Effect of calcination temperature on activation of catalyst

To optimize the activation temperature of catalysts, the Wittig reaction **(Scheme 1)** was performed using undoped nanocrystalline MgO heated at different activation temperatures. The undoped catalysts are heated at temperature 120, 450, 600, 700 and 900 °C and used further as catalyst. In our present study, we found that nanocrystalline MgO heated at 700 °C exhibits maximum catalytic efficiency (Fig. 10). The activity is less below the temperature 700 °C because active basic sites of MgO surface could have been possibly masked by adsorption of CO_2 and water vapors at lower temperatures. Accordingly, gradual increase of catalytic activity with increase in temperature is due to removal of CO_2 and water vapors from surface resulting into activation of MgO surface basic sites [44]. It is also observed that activation temperature of catalyst is different for different reactions [45]. Thermal activation of pure nanocrystalline MgO at 700°C exhibits smallest crystallite size as observed by XRD study. Whereas at temperatures above 700°C, catalytic activity decreases which may be attributable to increase in particle size and impurity influenced crystalline behavior [46]. Therefore, for further study, all doped and undoped catalysts are activated at 700°C prior to use in one pot Wittig reaction.

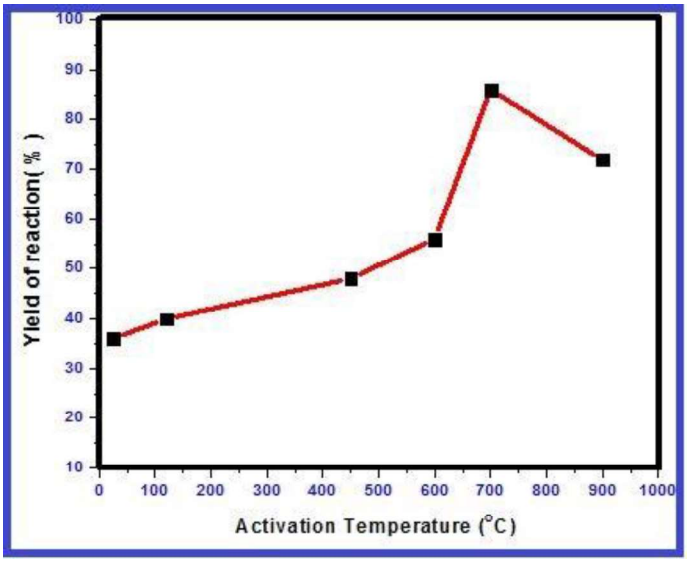

Fig. 10. Effect of temperature on activation of nanocrystalline MgO

3.7.2 Effect of Solvent

Catalytic efficiency of activated nanocrystalline MgO is obtained for different solvents in one pot Wittig reaction. It is observed that nanocrystalline MgO catalyst has maximum catalytic efficiency in polar aprotic solvent DMF with 81 % yield at room temperature, whereas, only 40 % yield has been obtained for toluene as solvent under the same reaction conditions (Table 3). Mechanism of reaction is well understood. During reaction, intermediates such as phosphonium salt, phosphorus ylide, betaine and oxa-phosphetane are formed. The polarity of solvent may play role in formation and stabilization of these intermediates. For this reason, more yield is observed with polar solvent while minimum yield is observed for non-polar solvent.

Table 3. Effect of solvent on catalytic activity of Nanocrystalline MgO in one pot Wittig reaction

Solvent	DMF	Acetonitrile	THF	Ethyl alcohol	Toluene	DMSO
% yield[a]	81	61	45	57	40	72

Reaction condition: 4.7 mmol benzaldehyde, 4.7 mmol TPP and 4.7 mmol ethyl bromo acetate are stirred with 200 mg nano MgO in each 5 mL solvent at RT, [a] isolated yield

3.7.3 Effect of doping of Cu, Fe and Mn on catalytic activity of MgO

Specific amount (200 mg) of activated catalyst was used for one pot Wittig reaction in DMF solvent. The end product ethyl cinnamate was characterized by TLC, HR-MS, ^{1}H-NMR and ^{13}C-NMR spectroscopic techniques. 1 wt% Mn doped MgO nanocatalyst shows better catalytic activity with 86% yield (Table 4, entry 6). Whereas only 56% yield is obtained for Fe doped MgO catalyst. Doping of Fe in MgO decreases the number and strength of basic sites (Table 4, entries 4). Undoped nanocrystalline MgO catalyst has 81% yield (Table 4, entry 3).It is more than that of commercial MgO and may be attributed to relative increase in the surface area and prismatic, hexagonal morphology of nanocrystalline MgO as observed in FE-SEM analysis. However, increase in particles size of Mn doped nanocrystalline MgO does not affect the yield due to more surface basicity by the virtue of surface donor properties of Mn due to its higher oxidation state (Stavale et al. 2012) as well as more number of low coordinated oxygen as observed in UV -DRS study. Cu doped MgO nanomaterial shows 70 % yield (Table 4, entry 5) which is lower than pristine nanocrystalline MgO due to decreased basicity, though it has more number of low coordinated oxygen at surface. Decrease in surface basicity of MgO is due to doping of Cu which decreases the strength of basic sites as observed by XPS [47]. One more reason for decrease in the catalytic activity of Cu doped MgO materials is incorporation of Cu metal in MgO lattice at high temperature heating required for activation. However, lower yield obtained for Fe doped MgO (Table 4, entry 3) may be due to formation of exchange bias layer of FeO on surface which decreases the number of low coordinated oxygen on surface and corners as expected due to heating at high temperature (Fan et al. 2013). Besides, doping of Fe in MgO increases the acidity due to small size of Fe (Ueda et al. 1985). The blank reaction is subjected to proceed without use of any catalyst. It shows no formation of olefin and triphenyl phosphonium oxide on TLC and isolated yield is 0 % (Table 4, entry 1) confirming the reaction is really a base catalysed.

Table 4. Effect of Cu, Fe and metal ion doping on catalytic activity of MgO

No	Catalysts	Reaction time/ Hr	Yield[a]/ %	Particle size Thickness(Length)	Morphology	E/Z ratio[b]
1	Blank reaction	24	0	--	--	--
2	Commerical MgO	12	60	1-2 micron	Irregular	99:1
3	Nanocrystalline MgO	12	81	18(68) nm	Hexagonal plates	95:5
4	1% Fe/MgO	12	56	32(240)nm	Hexagonal plates	99:1
5	1% Cu/MgO	12	70	70(450) nm	Hexagonal plates	96:4
6	1% Mn/MgO	12	86	21(>1000) nm	Nanosheets	95:5

[a]Reaction conditions: benzaldehyde (4.7 mmol), TPP (4.7 mmol) and ethyl bromo acetate (4.7 mmol) are stirred in 5 mL DMF with each catalysts at RT for 12 h stirring, [a] Isolated yield, [b]Entgegen /Zusammen ratio is calculated from integration lines in ^{1}H-NMR spectra of crude products after column chromatography

Thus, proposed one pot Wittig reaction revealed maximum yield of E-ethyl cinnamate for 1 wt% Mn doped nanocrystalline MgO. Further optimization of amount of precursors used in the Wittig reaction was carried out by keeping the same amount of catalyst and by varying the concentrations of the precursors under the same reaction conditions. After optimizing the precursors, amount of catalysts was also optimized using the optimized concentration of the precursors under the same reaction conditions.

- **Characterization of Wittig product**

HR-MS: [M +H] = 177.09 (calculated for $C_{11}H_{12}O_2$ - 176.21),

^{13}C-NMR:(500 MHz, $CDCl_3$) 14.38 δ, 60.35 δ, 118.31 δ, 128.02, 120.04 δ, 129.75 δ, 130.14 δ, 144.54.

3.7.4 Effect of Concentration of precursors and catalysts amount on catalytic activity of Mn doped MgO

Table 5 shows the effect of varying concentrations of benzaldehyde, triphenylphosphine, ethyl bromoacetate and catalysts amount on the catalytic activity of 1 wt% Mn doped MgO. On increasing the concentration of triphenylphosphine and ethyl bromo acetate from 1 to 1.2 equivalents, it shows negligible effect on rate and catalytic efficiency of the reaction (Table 5, entry 2). But on increasing the concentration of benzaldehyde from 1 to 1.5 equivalent, it affects the rate and catalytic efficiency drastically (Table 5, entry 3, 4). Under this optimized concentration of the reactants, catalyst amounts are varied from 200 mg to 50 mg. Best results are obtained in presence of 100 mg catalyst when we stirred 1.5 equivalent benzaldehyde with 1 equivalent of TPP and 1 equivalent of Ethyl bromo acetate (Table 5, entry 5).

Table 5. Effect of concentration of reactants and catalyst amount on catalytic activity of 1% Mn doped MgO

No	Reactants stichoimetry/ No of equivalents			Catalyst Amount/ Mg	Reaction Time/ h	Yield[a] %
	Benzaldehyde	TPP	Ethyl bromoacetate			
1	1	1	1	200	12	86
2	1	1.2	1.2	200	10	85
3	1.2	1	1	200	9	92
4	1.5	1	1	200	8	94
5	1.5	1	1	100	7	98
6	1.5	1	1	50	10	70

[a]Reaction conditions: 1 % Mn doped MgO activated catalyst is stirred with reactants in 5mL DMF solvent at RT. [a] isolated yield

We speculate that 1 wt% Mn doped nanocrystalline MgO is an eco-friendly and efficient catalyst for one pot Wittig reaction between 1.5 equivalent of benzaldehyde and 1 equivalent of triphenylphosphine with 1 equivalent of ethyl bromoacetate.

As shown in Table 5, entry 5 the presently reported 1 wt% Mn doped nanocrystalline MgO catalyst has 98% yield for 1.5 : 1 :1 of benzaldehyde, triphenylphosphine and ethyl bromoacetate precursors, respectively for 100 mg catalyst amount in DMF solvent at room temperature. The yield reported in this investigation is higher than that reported by Choudary et al. (Choudary et al. 2006) for nanocrystalline MgO. We also report that the catalyst ratio used in our approach is almost less than half than the earlier reported value.

3.7.5 Mechanistic study

The mechanism of Wittig reaction is well known under homogeneous condition. However, it is very interesting to see its mechanism on surface of catalysts under heterogeneous condition. Catalyst performs very important role firstly in providing acidic and basic sites for interaction with organic molecules for the formation of polar phosphonium salts, secondly deprotonation of phosphonium salts to form phosphorus ylides,

To confirm the above outcomes of mechanistic details, the intermediate phosphonium bromide salt was stirred with benzaldehyde in presence of catalyst (Scheme 2).

- **Reaction condition**

Phosphonium salt is stirred with benzaldehyde in presence of 100 mg catalysts in 5mL DMF solvent at RT

When 4.7 mmol of phosphonium salt was stirred with 4.7 mmols benzaldehyde in absence of catalyst, even after 15 h, only 3 % conversion of olefin was obtained (Table 6, entry 1).

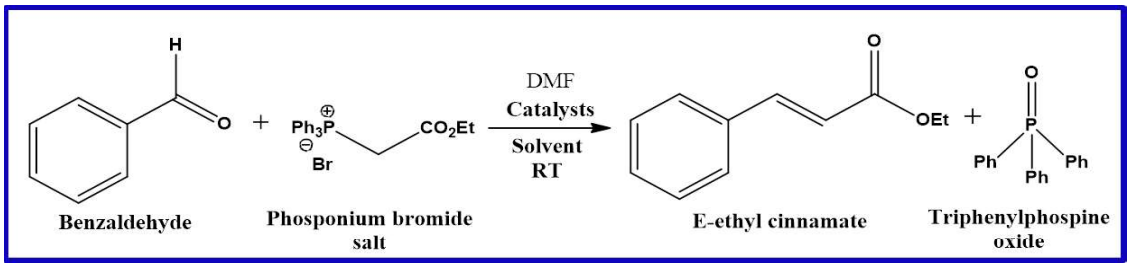

Scheme 2. Reaction of intermediate phosphonium bromide salt with Benzaldehyde

Table 6. Mechanistic investigation of one pot Wittig reaction by reaction with intermediate phosphonium salt

No	Reactants stoichiometry		Catalysts	Reaction Time/h.	Yield/ %
	Benzaldehyde	Phosphonium salt			
1	1	1	--	15	3
2	1	1	100 mg	10	95
3	1.2	1	100 mg	8	96
4	1.5	1	100 mg	6	98

It means that deprotonation of phosphonium salt is slow and hence the rate determining step of the reaction. After adjusting benzaldehyde stichoimetry from 1 to 1.5 equivalent, reaction proceeds with quantitative yield of 98 % within short period of time (Table 6, entry 4, 5). Based on these experiments, mechanism of on pot Wittig reaction is proposed on surface of catalyst (Scheme 3). In reactions, different types of charged intermediates are formed such as betaine, oxaphosphetane etc. after nucleophilic addition of polar phosphorane to benzaldehyde. Surface of catalysts is responsible for stabilization and formation of these intermediates. Finally oxaphosphetane intermediate collapses into products. Catalysts and products are separated by centrifugation and catalyst is activated for the next cycle of reaction.

Thus, we have enhanced the basicity of nanocrystalline MgO catalyst by doping transition metal Mn for the effective use in the one pot Wittig reaction. Our methodology is eco-friendly and easy to scale up for the different types of Wittig reactions. We also supported the mechanism of reactions by changing the concentration of reaction precursors and studied the same reaction in two steps

3.6.6 Recycling study

Fig. 11 presents the recycling data of nanocrystalline 1 wt% Mn doped MgO catalyst under the optimized reaction conditions. The catalyst is recycled five times without significant loss in the catalytic activity with almost the same recovery. After each cycle, catalyst was separated by simple centrifugation and washed with DMF and ethyl acetate. For each cycle, the separated catalysts again reactivated by heating at 700 $^{\circ}$C and reused for the next cycle of Wittig reaction. The phase and purity of 1% Mn doped MgO as catalyst is studied before and after reaction using XRD technique which substantiates that no significant change has been observed in phase and purity of catalyst.

In nutshell, we have demonstrated novel approach to obtain high yield for Wittig reaction compared to other MgO based catalysts. The effect of particle size, morphology and dopant material of catalyst was successfully studied for the reported reactions. Mn doped MgO catalyst was found to be an efficient catalyst to proposed reaction.

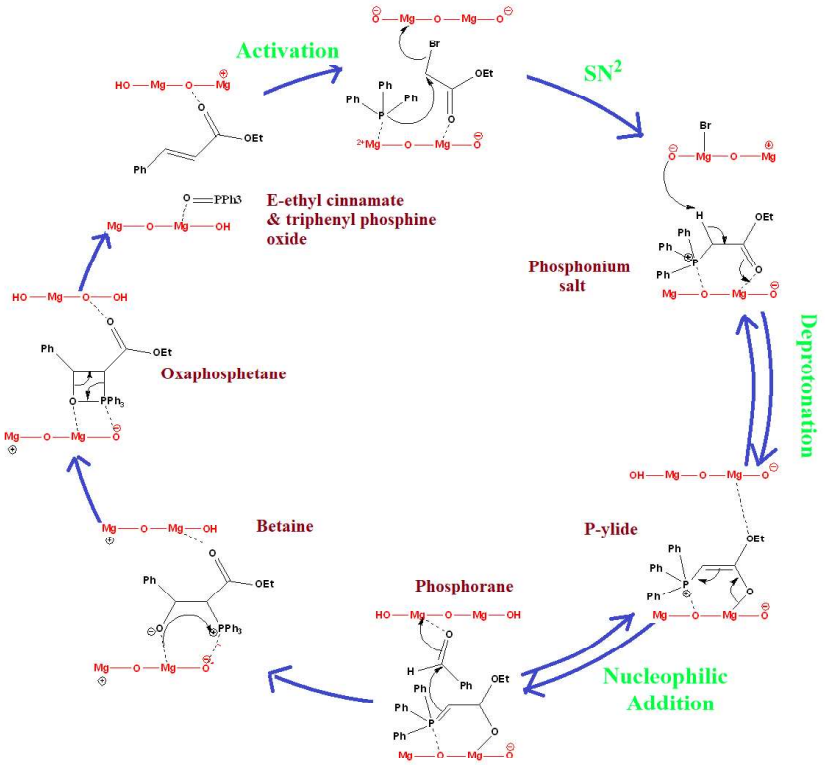

Scheme 3. Proposed mechanism of one pot Wittig reaction on surface of MgO catalyst

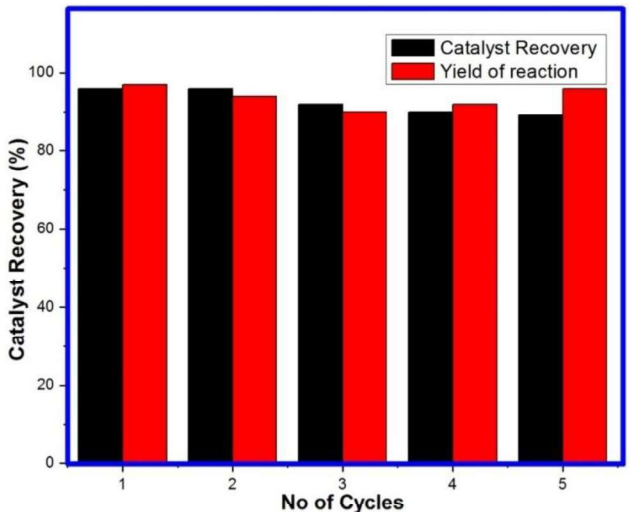

Fig. 11. Recycling of 1 wt% Mn doped MgO catalyst

4. CONCLUSIONS

Nanocrystalline catalytic systems comprising undoped MgO as well as Cu, Fe and Mn doped MgO in phase pure cubic form were synthesized using alkali leached hydrothermal method. The synergistic effect of doping of transition metal ions particle size and morphology in surface basicity enhancement of nanocrystalline MgO was investigated for the Wittig reactions. Doping of Cu in MgO increases the

number of basic sites but decreases the strength of this basic sites, while doping of Fe in MgO decreases both number and strength of basic sites on surface of MgO. Doping of Mn increases the number and strength of basic sites while Oxidation state of Mn in doped MgO plays an important role in order to enhance the catalytic activity. It is largely attributed to enhancement of surface basicity. The Mn doped MgO is found to be an efficient recyclable catalyst compared to its Fe and Cu doped counterparts in reported Wittig reaction for ethyl cinnmate preparation. One pot Wittig reaction is reported for Cu, Fe and Mn doped nanocrystalline MgO under the optimized reaction conditions of activation temperature, solvent and concentration of precursors. We believe that our methodology is green chemical for synthesis of E-ethyl cinnamate using transition metal doped nanocrystalline MgO catalysts in one pot Wittig reaction

ACKNOWLEDGEMENT

Dr. Mansur Moulavi sincerely thanks to Dr. B. B. Kale -Director, C-MET (Pune), Dr. Sudhir Arbuj C-MET (Pune) for providing characterization facilities. The authors extend their appreciation to the Deanship of Scientific Research at King Saud University for funding this work through research group No (RG-1440-093).

COMPETING INTERESTS

Authors have declared that no competing interests exist.

REFERENCES

1. Moulavi MH, Kale BB, Bankar D, Amalnerkar DP, Vinu A, Kanade KG. Green synthetic methodology: An evaluative study for impact of surface basicity of MnO2 doped MgO nanocomposites in Wittig reaction J. Sol. St. Chem. 2019;269:167-174.
2. Raina AP, Abraham Z. Chemical profiling of essential oil of *Kaempferia galangal* germplasm from India Journal of Esssential Oil Research. 2016;28:1-5.
3. Marvel CS, King WB. Ethyl cinnamate. Organic Syntheses. 199;9:38.
4. Saha M, Das AR. Nanocrystalline ZnO: A Competent and Reusable Catalyst for the Preparation of Pharmacology Relevant Heterocycles in the Aqueous Medium. Current Green Chemistry. 2020;7:53-104.
5. Hattori H.Solid base catalysts: Generation of basic sites and application to organic synthesis. Appl Catal A-Gen. 2001;222(1-2):247-259.
6. Lucrecia, A, Jesu's, H, Alberto, M, Jose MM, Francisco JU. Sustainable C-C bond formation through Knoenvengal reaction catalyzed by MgO-based catalysts. Reac. Kinet. Mech. 2016; 118(1):247-265.
7. Drexler MT, Amiridis MD. The effect of solvent on the heterogeneous synthesis of flavones over MgO. J. Catal. 2003;214(1):136-145.
8. Shinde ST, Kanade KG, Karale BK, Amalnerkar DP, Thorat NM, Arbuj SS, Kunde SP. Nanosized ZnO under solvent free condition: A smart and ecofriendly catalyst to microwave assisted synthesis of 3,4-dihydropyromidin-2(1H)-ones/thiones. Current smart materials. 2016; 1(1):68-66.
9. Gholinejad M, Bahrami M, Nájera C, Biji Pullithadathil B. Magnesium oxide supported bimetallic Pd/Cu nanoparticles as an efficient catalyst for Sonogashira reaction. J. Catal. 2018; 363:81-91.
10. Gholinejad, M, Bahrami, M., Nájera, C., Biji Pullithadathil, B., Magnesium oxide supported bimetallic Pd/Cu nanoparticles as an efficient catalyst for Sonogashira reaction. J. Catal. 2018; 363:81-91.
11. Kunde SP, Kanade KG, Karale KB, Akolkar HN, Randhavanae PV, Shinde ST. Synthesis and characterization of nanostructured Cu-ZnO: An efficient catalysts for the preparation of (E)-3-styrylchromone.
http://dx.doi.org/10.1016/j.arabjc.2016.12.015.
12. Babaie M, Sheibani H. Nanosized magnesium oxide as a highly effective heterogeneous base catalysts for rapid synthesis of pyranopyrazole via a tandem four component reaction. Arab. J. Chem. 2011;4(2):159-162.

13. Nicolaou KC, Harter MW, Gunzner JL, Nadin A. The Wittig and related reactions in natural product synthesis. Liebigs Ann. 1997;(7):1283-1301.
14. Taber DF, Nelson CG. Potassium hydride in paraffin: A useful base for organic synthesis. J. Org. Chem. 2006;71(23):8973-8974.
15. Moison H, Taxier-Boullet F, Foucad A. Knoevenagel, Wittig and Wittig-Horner reactions in presence of magnesium oxide or zinc oxide. Tetrahedron. 1987;43(3):531-542.
16. Choudhari BM, Mahendar K, Kantam ML, Ranganath K, Athar T. The one pot–Wittig reaction: a facile synthesis of α,β-unsaturated esters and nitriles by using nanocrystalline MgO. Adv. Synth. Catal. 2006;348(14):1977-1985.
17. Menezes OA, Silva PS, Hernandez EP, Borges LEP, Fraga MA. Tuning surface basic properties on nanocrystalline MgO by controlling preparation condition. Langmuir. 2010; 26(5):3382-3387.
18. Hattori H. Heterogeneous basic catalysis, Chem. Rev. 1995;95(3):537-558.
19. Kantam ML, Shiva Kumar, KB, Balasubramanyam V, Venkanna GT, Figueras F. One pot Wittig reaction for the synthesis of α,β-unsaturated esters using highly basic magnesium/lanthanum mixed oxide. J Mol Catal A Chem. 2010;321:10-14.
20. Gholinejad M, Firouzabadi H, Bahrami M, Nájera C. Tandem oxidation–Wittig reaction using nanocrystalline barium manganate ($BaMnO_4$); an improved one-pot protocol. J. Catal. 2018; 363:81-91
21. Kantam ML, Pal U, Sreedhar B, Choudary BM. An efficient synthesis of organic carbonates using nanocrystalline magnesium oxide. Adv. Synth. Catal. 2007;349:1671-1675.
22. Di Cosimo JI, Diez, V. K., Ferretti, C., Apesteguia. 2014. Basic catalysis on MgO: Generation, Characterization and catalytic properties of active sites. Chapter 1. Catalysis 26(26), 1-28. Royal Society of Chemistry.
23. Wu MC, Goodman DY. Acid/base properties of MgO studied by high energy resolution electron loss spectroscopy. Catalysis Letters. 1992;15(1):1-11.
24. Corma A, Iborra S. Optimization of alkaline earth metal oxide and hydroxide catalysts for base catalyzed reactions. Adv. Catal. 2006;49:239-302.
25. Zhang J, Wu Y, Li L, Wang X, Zhang Q, Zhang T, Tan Y, Han Y. Ti-SBA-15 supported Cu-MgO catalyst for synthesis of isobutyraldehyde from methanol and ethanol. RSC Adv. 2016;6:85940.
26. Stavale F, Shao X, Nilius N, Freund HJ, Prada S, Livia GM, Pacchioni G. Donor characteristics of transition metal doped oxides: Cr doped MgO versus Mo doped CaO. J. Am. Chem. Soc. 2012;134(128):11380-11383
27. Ueda W, Yokoyama T, Moro-oka Y, Ikawa T. Enhancement of surface base property of magnesium oxide by combination of metal ion. Chemistry Letters. 1985;14(7):1059-1062.
28. Ding Y, Zhang G, Wu H, Hai B, Wang L, Qian Y. Nanoscale magnesium hydroxide and magnesium oxide powders: Control over size, shape, and structure via hydrothermal synthesis. Chem. Mater. 2001;13(2):435-440.
29. Lee DW, Park YM, Lee KY. Heterogeneous Base Catalysts for Transesterification in Biodiesel Synthesis. *Catal. Surv. Asia.* 2009;13:63–77.
30. Coluccia S, Tench AJ, Surface structure and surface state and surface state in magnesium oxide powders. J. Chem. Soc. Faraday Trans. 1979;75(0):1769-1779.
31. Zhang M, Gao M, Chenab J, Yu Y. Study on key step of 1,3-butadiene formation from ethanol on MgO/SiO_2. RSC Adv. 2015;5(33):25959.
32. Hattori H. Solid base catalysis: Generation, Characterization and catalytic behavior of basic sites. Journal of the Japan Petroleum Institute 2004;47(2):67-81.
33. Fan Y, Smith, KJ, Lupke G, Hanbicki AT, Goswami R, Li CH, Zhao HB, Jonkar BT. Exchang bias of the interface system at Fe/MgO interface. Nat. Nanotechnol. 2013;8:438-444.
34. Hadia N, Mohamed H. Characteristics and optical properties of MgO nanowires synthesized by solvothermal method. Mater. Sci. Semicond. Process. 2015;29:238-244.
35. Raman CV. The vibration spectra of crystals-Part IV. Magnesium oxide. Proc. Indian Acad. Sci. A. 1947;26:383-390.
36. Raman CV. The vibrations of MgO crystal structure and its infrared absorption spectrum. Proc. Indian Acad. Sci. A. 1961;54:205-222.
37. Philippt R, Fujimoto K. FTIR spectroscopic studies COP adsorption/Desorption on MgO/CaO catalysts. J. Phys. Chem. 1992;96(22):9035-9038.
38. Vasquez RP, CuO by XPS. Surf. Sci. *Spectra*. 1998;5:265-266.

39. Vedrine JC. Acid–base characterization of heterogeneous catalysts: an up-to-date overview, *Res Chem Intermed*, *1998;41(12):9387–9423.*
DOI: 10.1007/s11164-015-1982-9.
40. Mansour AN, Brizzolara RA. Characterization of the Surface of FeO Powder by XPS, *Surf. Sci. Spectra* 1996;4:345-350.
41. Nesbitt, HW, Banergee D. Interpretation of XPS Mn(2p) spectra of Mn oxyhydroxides and constraints on the mechanism of MnO_2 precipitation, Am. Mineral. 1998;83:305–315.
42. Stranick, MA. MnO_2 by XPS Surf. Sci. Spectra. 1999;6:31-38.
43. Tanabe K, Yamaguch T. Basicity and acidity of solid surfaces. Journal of the research institute for catalysis Hokkaido University. 1964;11(3):179-184.
44. Gadge ST, Mishra A, Gajenji AL, Shahi NV, Bhanage BB. Magnesium oxide as a heterogeneous and recyclable base for the N-methylation of indole and o-methylation of phenol using dimethyl carbonate as a green methylating agent. RSC Adv. 2014;4:50271.
45. Zhang M, Gao, M., Chenab, J., Yu, Y., 2015. Study on key step of 1,3-butadiene formation from ethanol on MgO/SiO_2. RSC Adv. 5(33), 25959.
46. Zhang X, Zheng Y, Feng X, Han X, Bai Z, Zhiping Zhang Z. Calcination temperature-dependent surface structure and physicochemical properties of magnesium oxide. RSC Adv. 2015;5:86102-85112. .
47. Pudi SM, Zoeb A, Biswas P, Kumar S. Liquid phase conversion of glycerol to propanediol over highly active Copper/Magnesia catalysts. J. Chem. Sci. 2015;127(5):833-842.

Biography of author(s)

Dr. Mansur Moulavi
Department of Chemistry, PDEA's Annasaheb Waghire College, Otur, Pune -412409, India.

He is working as an Assistant Professor of Chemistry in PDEA's Annasaheb Waghire College, Maharashtra, India. He completed Ph. D. in August 2020 under the guidance of Dr. K. G. Kanade. He has 13 years of academic experience at UG and PG level. His Research area focused on Synthesis and characterization of nanomaterial's for application in catalysis, gas sensing and agriculture. He is also working in solid state chemistry using computational chemistry. He published 08 research papers in international reputed journals. He is actively involved in academic writing, administrative and college committees.

Prof. Kaluram Kanade
Annasaheb Awate Arts, Commerce, Hutatma Babu Genu Science College, Manchar Pune-410503, India.

He was born in Maharashtra, India, 2nd June 1963. He is a Principal, Annasaheb Awate Arts, Commerce and Hutatma Babu Genu Science College, Manchar, Pune, India. He holds a Ph. D degree in Chemistry for the research from Pune University in 2007. His Ph.D Thesis has received G.C. Jain Thesis award by Material Research Society of India in 2008. He has received International Research Fellow award for one year at KRICT, Daejeon, South Korea in 2005, and he nominated for Commonwealth Fellowship. He has 31 years Undergraduate and Postgraduate teaching experience. His research interests include Nanomaterial Synthesis, Development of Visible Light Photocatalyst to Renewal of Hydrogen energy, Nanostructured catalyst to degradation of organic waste, Synthesis of ferrite materials, Gas sensor materials. Under his supervision four research scholars had completed Ph. D degree, one completed M Phil Degree and one Research scholars are pursuing research. He had been successfully shouldered various academic and administrative responsibilities. He had been worked five years (from 2015-2020) as Director at Yashavantrao Chavan Institute of Science (Autonomous), Satara, Maharashtra, India.

DISCLAIMER
This chapter is an extended version of the article published by the same author(s) in the following journal.
Arabian Journal of Chemistry, 14, 103134, 2021.